Enhanced Selectivity in Scheelite–Calcite Flotation Using Oleic and Palmitic Acid Mixed Collectors: Experimental and Molecular Dynamics Insights

Surya Kanta Das[a, b], Pravanjani Swain[a, b], Shivakumar I. Angadi[a, b], Swagat S. Rath[*,a, b]
[a]CSIR-Institute of Minerals and Materials Technology, Bhubaneswar, India
[b]Academy of Scientific and Innovative Research (AcSIR), Ghaziabad - 201002, India

Abstract

The flotation separation of scheelite from calcite remains a significant challenge in mineral processing due to their similar surface characteristics. The present study proposes a novel approach using a 1:1 mixture of oleic acid and palmitic acid as a mixed collector to achieve effective separation. The mixed collector system enriched the WO_3 content from 0.19% in the feed to 2.2% in the float fraction, with an overall recovery of approximately 81.2% in a single flotation stage. In comparison, calcite recovery was as low as 26.8%, supporting the scheelite selectivity of the mixed collector system. Additionally, the flotation mechanism, involving the interaction between collector species and mineral surfaces, was investigated using Fourier transform infrared spectroscopy, UV–vis diffuse reflectance spectroscopy and X-ray photoelectron spectroscopy. The results revealed that adsorption under the mixed collector system facilitated the formation of a greater number of Ca-carboxylate complexes on the scheelite surface than on calcite, indicating preferential adsorption on scheelite. Moreover, the molecular dynamics simulation results suggested that the mixed collector system exhibited the maximum water-displacing ability and the highest accumulation of collector molecules on the scheelite (1 1 2) surface, compared to both collectors used individually.

Keywords: Scheelite, calcite, flotation, fatty acids, palmitic acid, MD simulation

* Communicating Author: ssrath.immt@csir.res.in, Tel. No.: +91-674-2379147; Fax No: +91-674-2581160

1. Introduction

The global depletion of WO_3 grades in wolframite deposits has led to a 40% share of global tungsten production being derived from scheelite, despite the associated beneficiation challenges (Das et al., 2023a). Scheelite, a calcium tungstate mineral ($CaWO_4$), commonly occurs in association with other calcium-bearing minerals such as calcite, fluorite, and apatite. Froth flotation is a key technique employed for the beneficiation of scheelite. However, the association of calcium-bearing impurities, especially calcite, poses significant challenges in effectively concentrating scheelite particles (Dong et al., 2018; He et al., 2025). The selective adsorption of collectors on mineral surfaces plays a crucial role in enabling flotation separation, and this selectivity depends on differences in surface characteristics between valuable and gangue minerals. In the case of scheelite and calcite, both minerals possess similar cationic charge (Ca^{2+}) and thus exhibit identical Ca-active sites on their commonly exposed surfaces. Moreover, scheelite and calcite exhibit similar solubility, and the anionic groups of both minerals (WO_4^{2-} and CO_3^{2-}, respectively) are nearly identical in size (Wei et al., 2023). Consequently, calcite responds similarly to scheelite during flotation and reports to the froth product, leading to dilution of the concentrate grade. This, in turn, increases the cost of downstream processing (Gao et al., 2020). Hence, it is crucial to study the adsorption behaviour of different collectors and develop effective collector systems capable of selectively floating scheelite particles.

Oleic acid is a conventional fatty acid collector widely used in the flotation of scheelite due to its strong collecting ability, low cost, and non-toxic nature (Peng et al., 2024; Guan et al., 2024; Zhu et al., 2025). The carboxyl group of oleic acid interacts with calcium ions on the scheelite surface via its oxygen atoms, leading to the formation of calcium oleate precipitates that impart hydrophobicity. However, oleic acid does not differentiate between scheelite and calcite surfaces and adsorbs on calcite in a similar manner (Kang et al., 2019). As a result, flotation using oleic acid lacks selectivity, which has motivated researchers to explore various co-collectors. The synergistic use of collectors enhances both the collecting ability and selectivity of the flotation system (Kupka and Rudolph, 2017; Yan, 2018; Foucaud et al., 2021; Das et al., 2023a; Peng et al., 2024). Nevertheless, such development would also avoid the energy-intensive

Petrov process, which requires heating the flotation pulp to about 80 °C to desorb collector molecules from calcite surfaces (Foucaud et al., 2022).

Various fatty acid collectors, such as stearic acid, linoleic acid, and myristic acid, have been studied as alternatives to oleic acid for the selective flotation of scheelite. However, myristic acid offers poor floatability due to its short chain length, whereas linoleic and stearic acids provide a better balance between collecting ability and selectivity (Foucaud et al., 2022). Similarly, the use of myristic acid ($C_{14}H_{28}O_2$) and mandelic acid ($C_8H_8O_3$) is also reported in various mineral flotation processes. α-bromo-myristic acid has recently gained popularity in selectively collecting spodumene over albite, quartz and other associated gangue minerals (Cook et al., 2023; Li et al., 2025). More recently, the structural modification of oleic acid, as well as sodium oleate, has been investigated to improve selectivity. Chen et al. (2025 & 2026) synthesized α-bromooleic acid (DBOA) by substituting Br at the α-position of sodium oleate. Later, the authors complexed DBOA with Ca(II) ions, which further improved both selectivity and collecting ability. In addition, mixtures of fatty acid collectors, such as oxidized paraffin soap (OPS), tall oil fatty acids (TOFA), and fatty acid alcohols, have also been tested in scheelite flotation (Filippov et al., 2019; Wu et al., 2022; Foucaud et al., 2022; Wei et al., 2023). OPS, a mixture of C12–20 fatty acids, is widely used in industrial scheelite flotation plants because of its low cost and strong collecting and foaming properties. However, OPS shows poor selectivity at lower pulp temperatures (Wu et al., 2022). Similarly, the performance of commercial TOFA depends on the proportion of saturated fatty acids (Foucaud et al., 2022). Fatty acid alcohols, such as isotridecanol, have also demonstrated promising selectivity toward scheelite.

Despite these advancements, the fundamental adsorption mechanisms of fatty acid collectors on scheelite and calcite remain unclear, particularly for alternative fatty acids that may provide improved selectivity. Palmitic acid ($C_{16}H_{32}O_2$) is one such potential option. Recent studies have shown its potential as a co-collector with oleic acid in apatite flotation, where it improved flotation selectivity (Oliveira et al., 2019; Santos et al., 2022). Furthermore, Filippov et al. (2018) reported the use of palmitic acid

as a collector for the scheelite ore of the Tabuaco deposit, where experimental results demonstrated that palmitic acid induces better selectivity towards scheelite than fluorite. However, the use of palmitic acid as a co-collector in scheelite flotation, and its adsorption behaviour on scheelite and calcite surfaces, has remained largely unexplored. In addition, the literature provides very limited systematic information on the application of mixed collector systems comprising both saturated and unsaturated fatty acids in the scheelite–calcite flotation system. Therefore, it is essential to investigate selective and novel collector combinations and to develop a fundamental understanding of the influence of hydrocarbon chain structures and synergistic interactions on the selective adsorption of scheelite over calcite.

In view of this, the present study investigates the potential application of palmitic acid as a co-collector with oleic acid for the selective flotation of scheelite from calcite. Laboratory-scale flotation experiments were conducted on Hutti gold mine tailings containing scheelite, and the results were integrated with molecular dynamics (MD) simulations to assess collector adsorption behaviour under different conditions. To further validate the adsorption mechanisms, systematic studies were performed on pure scheelite and calcite minerals using Fourier Transform Infrared Spectroscopy (FTIR), UV–Vis Diffuse Reflectance Spectroscopy (UV-Vis DRS), and X-ray Photoelectron Spectroscopy (XPS). The outcomes of this work provide new insights into the synergistic role of oleic acid and palmitic acid in scheelite flotation and establish a novel and potentially useful collector system for industrial applications.

2. Materials and methods

2.1. Minerals and reagents

The feed material used in the present investigation is gold mine tailings sourced from the Hutti gold mine in the Raichur district of Karnataka, India. The bulk sample details and feed characteristics are described in earlier publications that exclusively discussed the potential of pre-concentrating scheelite particles using a Falcon concentrator (Das et al., 2023a, b, & c). In the present investigation, flotation studies were carried out on the gravity concentrates obtained from the Falcon concentrator. Particle size analysis was performed using a laser light-scattering particle size analyzer (Make: Malvern,

Model: Mastersizer 3000E). Fig. 1 shows the particle size distribution of the flotation feed sample, indicating d_{80} and d_{50} values of about 96 µm and 58 µm, respectively. Table 1 shows the major oxides analyzed using X-ray fluorescence spectroscopy (XRF, Make: PANalytical, Model: Zetium) present in the flotation feed. Notably, the WO_3 content was determined through Inductively Coupled Plasma Optical Emission Spectrometry (ICP-OES). It is observed that the flotation feed contains approximately 0.19% WO_3, with SiO_2 being the major constituent, accounting for approximately 53.5%. The feed material also contains substantial amounts of Fe_2O_3, CaO, and MgO.

Table 1. Chemical analysis of the flotation feed

Elements	*WO_3	As_2O_3	Fe_2O_3	MnO	TiO_2	CaO	K_2O	SO_3	P_2O_5	SiO_2	Al_2O_3	MgO	Na_2O	LOI
%	0.19	2.94	10.33	0.10	1.01	8.91	0.94	2.02	0.16	49.25	10.74	4.44	1.97	7.2
*WO_3 analysis was performed using ICP-OES														

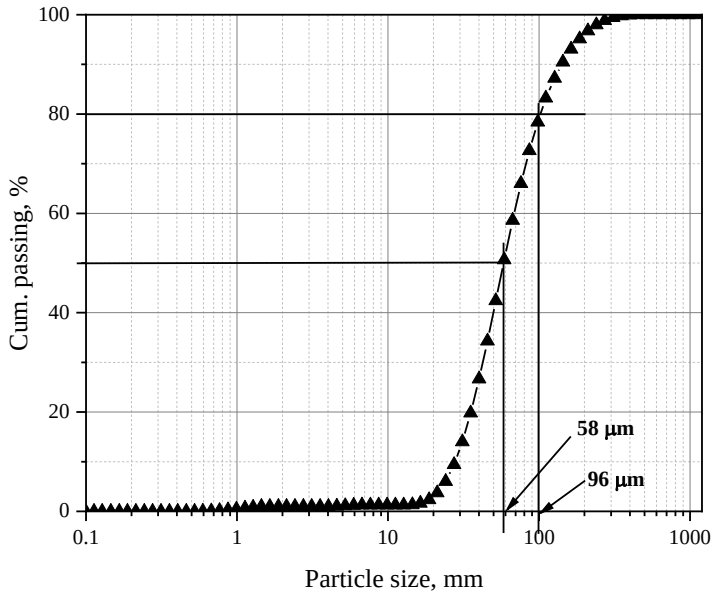

Fig. 1. Particle size analysis of the flotation feed

The lab-scale adsorption studies were conducted on commercially available pure scheelite and calcite mineral samples. The X-ray diffraction (XRD, Make: PANalytical, Model: X'pert Pro) technique was used to analyze the purity of the samples, and the obtained spectra are presented in Fig. 2. The XRD patterns of the pure mineral samples confirm the purity of the sample and thus make it suitable for single mineral adsorption studies.

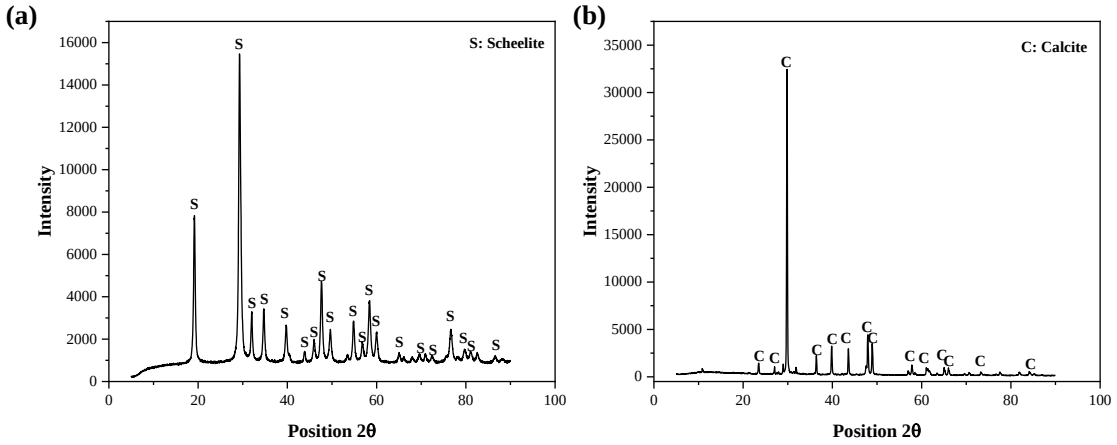

Fig. 2. XRD analysis of pure mineral samples (a) scheelite, (b) calcite

Analytical-grade oleic acid and palmitic acid served as collectors, while hydrochloric acid (HCl) and sodium hydroxide (NaOH) were employed as pH regulators. Methyl isobutyl carbinol (MIBC) was used as the frother, and deionized water was utilized in all experiments.

2.2. Flotation tests

Laboratory-scale flotation experiments were carried out using a Denver flotation cell. The feed pulp was prepared by thoroughly mixing the feed sample with deionized water, maintaining a solid concentration of 20% (w/w). The slurry was agitated at an impeller speed of approximately 1500 rpm to ensure proper mixing. The collectors and frother (MIBC) were added at predefined dosages and conditioned for 5 min and 2 min, respectively. The dosage of MIBC was fixed at 200 g/t throughout all the experiments. After completion of conditioning, the air valve was opened, and the froth was collected using a scrapper. Both froth and non-froth samples were dewatered, dried, weighed and chemically analyzed to calculate yield and recovery.

2.3. FTIR Spectroscopy

Pure calcite and scheelite samples (5g each) were mixed with 20 ml of deionized water in order to maintain a pulp density similar to that followed in the flotation experiments. Further, the slurry was conditioned with oleic acid, palmitic acid, and their 1:1 mixture, while maintaining a total dosage of 100g/t, using a magnetic stirrer.

Later, the samples were filtered and dried in the oven, then analyzed with a Bruker Alpha II instrument (400–4000 cm^{-1}) using KBr disc pellets.

2.4. UV-Vis DRS

The UV-Vis DRS spectroscopy was conducted using a UV-Vis spectrophotometer (Make: Agilent, Model: Carry 5000). For each analysis, 5g of pure scheelite and calcite samples were conditioned with oleic acid, palmitic acid and their 1:1 mixture as mentioned in section 2.3. The UV-Vis spectra of the filtered solid samples were analyzed keeping $BaSO_4$ as refrence sample.

2.5. XPS

XPS analysis was conducted using a Thermo Fisher Nexsa instrument (Model:). Pure scheelite and calcite samples were conditioned under different reagent systems, similar to the FTIR sample preparation process described in section 2.3. Later, polyvinyl alcohol (PVA) was used as a binder for preparing sample pellets. The spectra were recorded using Al Kα radiation with a hemispherical energy analyzer, and the binding energies of the samples were determined from the acquired spectra.

2.6. Computational settings

The present study utilized Biovia Materials Studio 2024 software to perform MD simulations (Clark et al., 2005; Segall et al., 2024). The unit cell of scheelite was geometry-optimized using plane-wave density functional calculations with the CASTEP module. The Generalized Gradient Approximation (GGA) with the Perdew–Burke–Ernzerhof (PBE) functional was employed, using an energy cutoff of 500 eV and ultrasoft pseudopotentials. The optimized unit cell was cleaved along the (112) plane, which is the most stable and commonly reported cleavage plane of scheelite (Kupka and Rudolph, 2017). A supercell of dimensions 59.83 Å × 55.16 Å × 39.81 Å was constructed, consisting of three atomic layers representing the surface slab of scheelite (112) (Fig. 3). The surface structure was further geometry optimized using the Forcite module with the Universal Force Field (UFF) before the MD simulations.

Fig. 4 presents the anionic forms of oleic acid and palmitic acid, which were geometry-optimized using the CASTEP module. The present study considered 14 reagent

molecules and 4000 water molecules for the MD simulations. Fig. 5 presents a typical ensemble of scheelite (112)-collector-water system used for the simulation. The MD simulations were conducted in the NVT ensemble using the Nose–Hoover thermostat at 298 K, with a time step of 1 fs and a total simulation time of 500 ps. The simulation aimed to determine the concentration profiles of collector and water molecules near the scheelite surface, using both reagents and their combination, to generate molecular-level insights into the adsorption behaviour of the collector molecules on the scheelite (112) surface.

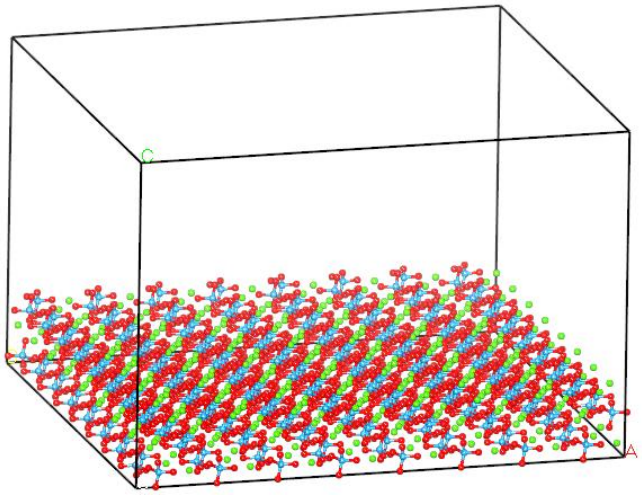

Fig. 3. Optimized supercell of scheelite (112) consisting of three layers

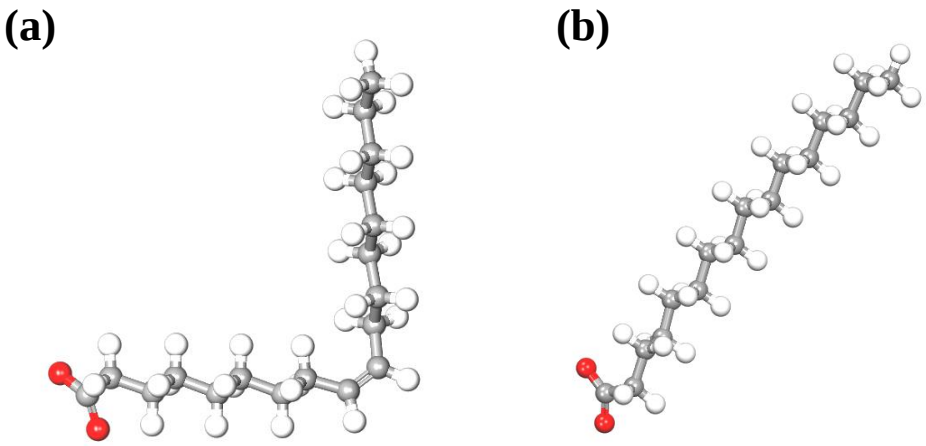

Fig. 4. Optimized structures of (a) oleic acid, (b) palmitic acid

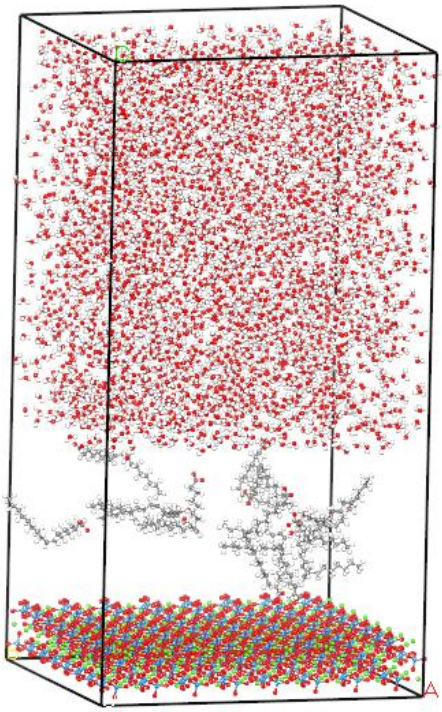

Fig. 5. Typical MD configuration of scheelite (112)-collector-water system before running the simulation

3. Results and discussion

3.1. Flotation

3.1.1. Influence of pH in scheelite flotation

Pulp pH has a significant impact on the floatability of scheelite as well as calcite (Kupka and Rudolph, 2017; Yang, 2018; Das et al., 2023). Therefore, initial studies were conducted to assess the effect of pH on the floatability of scheelite and calcite using oleic acid as the collector at a dosage of 100g/t. The pulp pH was varied from 6 to 10, and the froth products were collected at different time intervals, ranging from 20 s to 360 s. The collection and analysis of froth products at various time intervals would enable the determination of the flotation collection time, as well as provide insights into the flotation behaviour of both scheelite and calcite.

Fig. 6 depicts that both scheelite and calcite show good floatability at pH 10. The cumulative recovery of scheelite increased from 63.5% at pH 6 to 92.6% at pH 10. Such a substantial gain in scheelite recovery can be attributed to the stability of scheelite at

alkaline pH and to the increased ionization of oleic acid at higher pH. Scheelite, a salt-group mineral, is sparingly soluble in aqueous media at acidic pH (Wei et al., 2023). At pH < 6, scheelite possesses a high tendency for surface dissolution, resulting in the formation of H_2WO_4 (tungstic acid) and HWO_4^- ions. The presence of these species on the scheelite surface inhibits the adsorption of oleic acid, limiting its floatability. On the other hand, at pH values greater than 8, oleic acid ionizes more, providing more carboxylate ions (RCOO-), thereby enhancing particle-to-collector interactions. Moreover, the adsorption of oleic acid takes place through its carboxylate ions ($RCOO^-$) coordinating with the cationic sites (Ca^{2+}) ions present in the scheelite surface (Kupka and Rudolph, 2017). At alkaline pH, the concentration of Ca^{2+} ions remains relatively constant over a wide pH range, providing active sites for collector adsorption (Gao et al., 2016; Wei et al., 2023). Therefore, the majority of industrial-scale scheelite flotation is carried out at pH ~9-10 (Han et al., 2017; Dhar et al., 2020; Foucaud et al., 2022).

The flotation of calcite also follows a similar trend, with the cumulative recovery increasing from 55.5% to 91.3% as the pH increases from 6 to 10. Calcite, also a salt-type mineral, is sparingly soluble in aqueous solution depending on pH. Calcite releases Ca^{2+} ions into the pulp at acidic pH due to a protonation reaction. As a result, HCO_3^- ions are deposited on the calcite surface, which inhibits oleic acid from adsorbing on its surface (Faramarzpour et al., 2022). However, a further increase in pH to an alkaline medium promotes the ionization of oleic acid, which subsequently improves adsorption on the calcite surface (Dhar et al., 2020).

Interestingly, beyond 180s of flotation, there is hardly any improvement in scheelite recovery to the froth product. Therefore, 3 min of flotation time and a pulp pH of 10 were selected for future investigation.

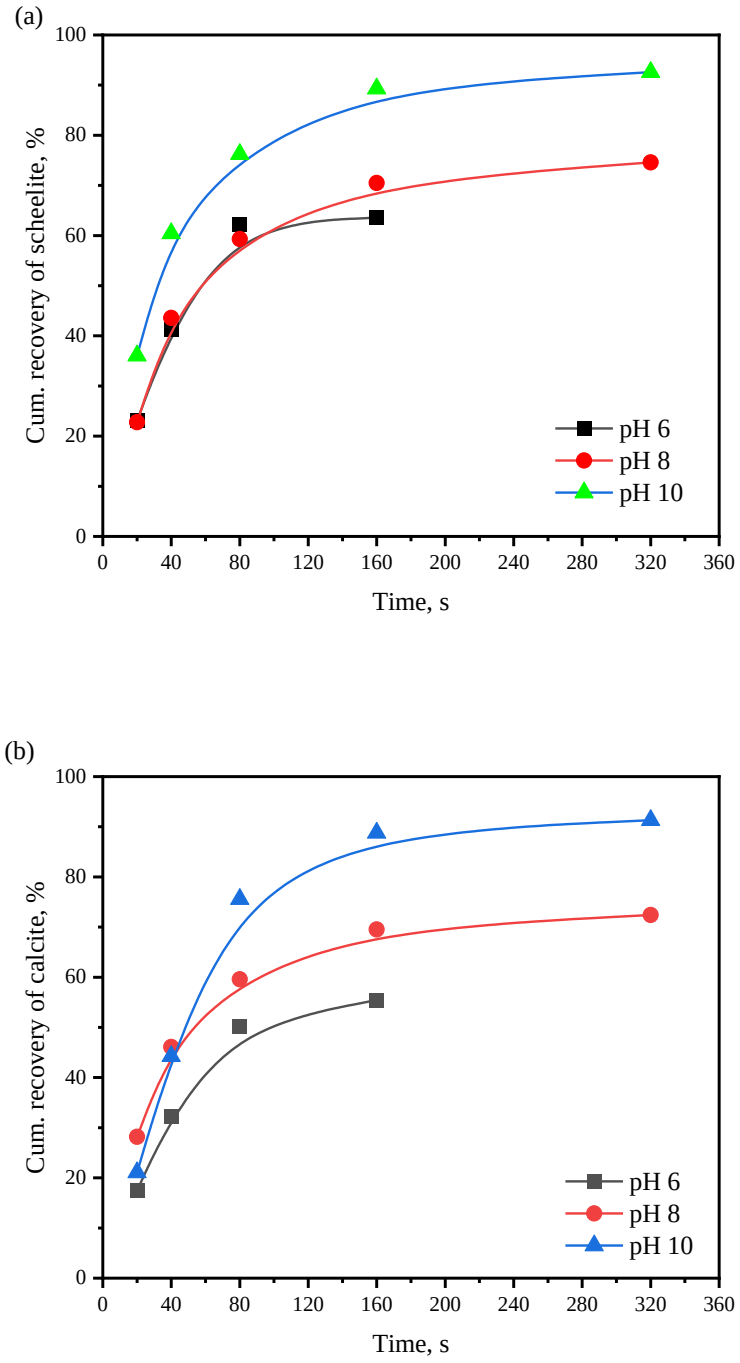

Fig. 6. Cumulative flotation recovery of (a) scheelite and (b) calcite with respect to pH

3.1.2. Selection of suitable fatty acid collectors

The primary objective of the present study is to investigate the flotation behaviour of scheelite particles under the action of different fatty acid-based collectors, such as oleic acid, mandelic acid, myristic acid and palmitic acid. The experiments were conducted

under identical flotation conditions to evaluate the effectiveness of each collector in selectively floating scheelite e particles. The flotation conditions were selected based on literature and our preliminary experimental studies (Das et al., 2025). All experiments were conducted at a pH of ~10, a pulp density of 20% (w/w), and with a fixed collector dosage of 100 g/t. The conditioning time for the collectors was maintained at 5 min.

The obtained results were used to construct the grade–recovery curve, as presented in Fig. 7, to compare the performance of the different collectors. It can be observed from the figure that oleic acid achieved the maximum recovery, while palmitic acid obtained the maximum WO_3 content, indicating better selectivity. Mandelic acid displayed intermediate flotation performance, whereas myristic acid demonstrated poor flotation response in terms of both grade and recovery. The flotation behaviour of each collector can be explained by its molecular structure, chain length, and degree of saturation, as these characteristics significantly affect its hydrophobicity and selectivity.

Fig. 7 depicts that oleic acid recovered about 92% of the scheelite values, with the WO_3 content increasing from 0.19% in the feed to 0.47% in the flotation concentrate. Oleic acid (C_{18}) is a monounsaturated fatty acid with a double bond at the 9th carbon, providing structural flexibility and enabling better molecular alignment and adsorption onto the scheelite surface. Moreover, its long hydrocarbon chain imparts sufficient hydrophobicity for efficient particle–bubble attachment (Kupka and Rudolph, 2017; Foucaud et al., 2021). In contrast, palmitic acid (C_{16}), a saturated fatty acid with a straight-chain structure, exhibited selective interaction with scheelite surfaces, resulting in a higher WO_3 content of 2.5% but a lower overall recovery. The straight-chain structure limits the solubility of collector molecules in the pulp, thereby reducing their adsorption on a larger number of particles. It is well reported that the solubility and mobility of fatty acid collectors increase with an increase in unsaturation levels (Leja, 1981; Filippov et al., 2018; Foucaud et al., 2019 & 2022). Mandelic acid, on the other hand, displayed moderate flotation performance with 0.49% WO_3 and about 51% recovery. The aromatic structure of mandelic acid

enhances its dispersibility in the pulp, whereas the presence of a hydroxyl (-OH) group in the structure increases its hydrophilicity, resulting in moderate overall floatability. Myristic acid (C_{14}) has a relatively short carbon chain and a high degree of saturation, resulting in the poorest flotation performance. Myristic acid, when used as a collector, recovered only 8.9% of the scheelite values, with a very minor enrichment in the concentrate grade (0.34%). A similar observation was reported by Foucaud et al. (2022), who noted that myristic acid exhibits a very low surface tension at the solid/air interface, thereby enhancing the hydrophilicity of scheelite particles and promoting particle-bubble detachment.

It indicates that both shorter chain length and aromatic structure hinder the induction of sufficient hydrophobicity required for scheelite flotation. In view of this, a combination of oleic acid and palmitic acid, representing unsaturated and saturated fatty acids, respectively, could provide a synergistic effect favouring scheelite flotation. The structural flexibility and long hydrocarbon chain of oleic acid could provide suitable collecting ability, whereas the saturated structure of palmitic acid could provide enhanced selectivity.

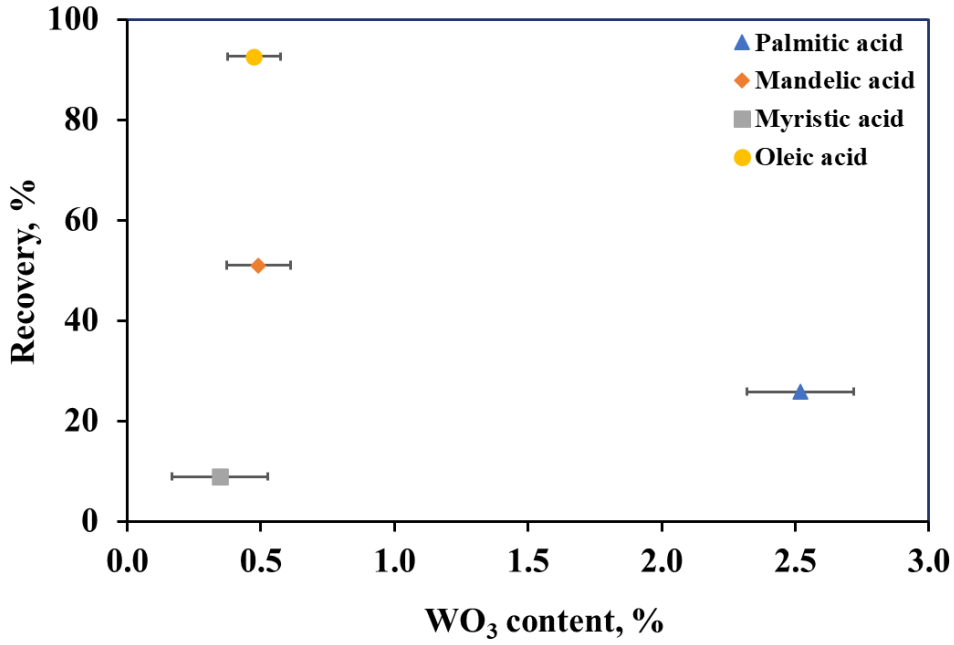

Fig. 7. Flotation performance (grade-recovery curve) of different fatty acids in scheelite flotation

3.1.3. Flotation response using a mixture of oleic acid and palmitic acid

The combined effect of oleic acid and palmitic acid was evaluated by varying their mixing ratios for the selective flotation of scheelite from calcite. The total collector dosage was fixed at 100 g/t, and the pulp pH was maintained at ~10. Fig. 8 illustrates the flotation recoveries of scheelite and calcite, as well as the corresponding WO_3 content as a function of the oleic acid-to-palmitic acid ratio varying from 4:0 to 0:4.

It can be observed from Fig. 8 that the recovery of both scheelite and calcite decreases with an increasing proportion of palmitic acid in the collector blend. Specifically, the recovery of scheelite decreased from 92.6% to 30.1%, while that of calcite decreased from 91.3% to 10.3% as the oleic acid-to-palmitic acid ratio changed from 4:0 to 0:4. This indicates that palmitic acid alone exhibits considerably weaker collecting ability compared to oleic acid. However, the decline in recovery is more pronounced for calcite than for scheelite.

In contrast, the WO_3 content in the flotation concentrate increased consistently with the increase in palmitic acid proportion, rising from 0.47% to 2.52% as the oleic acid-to-palmitic acid ratio decreased from 4:0 to 0:4. These findings align with the results presented in Section 3.1.2, where both collectors were tested individually. A higher proportion of oleic acid in the blend promotes greater scheelite recovery, whereas a higher palmitic acid content enhances selectivity. Notably, at an oleic acid-to-palmitic acid ratio of 1:1, scheelite achieved a recovery of approximately 81.2% with a WO_3 grade of 2.2%, while calcite recovery dropped sharply to around 26.8%. This demonstrates that the combined use of oleic and palmitic acids in equal proportions produces a synergistic effect, appropriate for maintaining a considerable balance between scheelite grade and recovery.

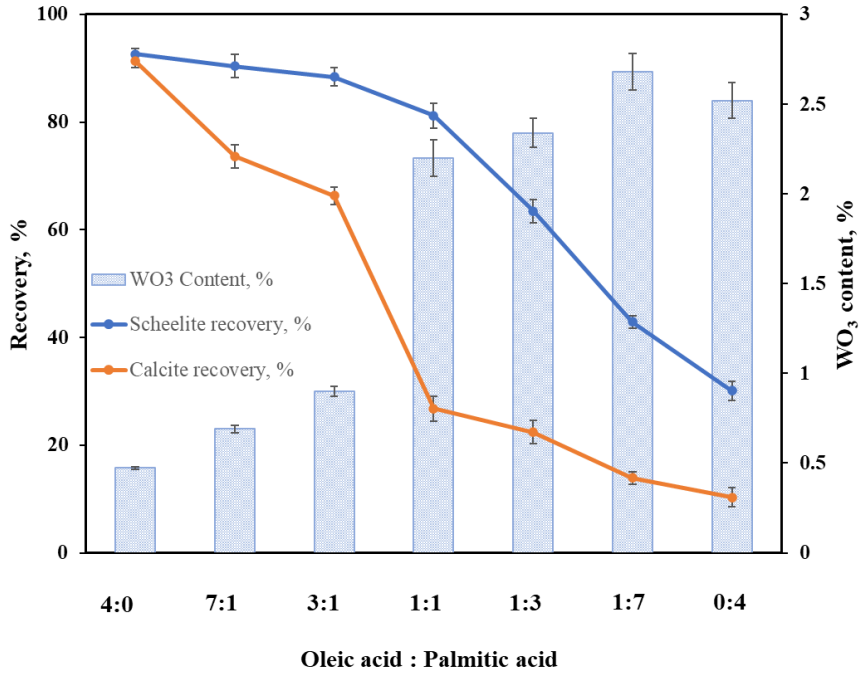

Fig. 8. Effect of oleic acid-to-palmitic acid ratio on WO_3 content, scheelite recovery and calcite recovery

3.2. FTIR analysis

The flotation behaviour of scheelite and calcite under the action of different collectors can be explained with the changes in their FTIR spectra before and after adsorption. Fig. 9 presents the IR spectra of both scheelite and calcite treated with (a) oleic acid, (b) palmitic acid, and (c) an oleic acid–palmitic acid mixture (1:1).

The characteristic bands at 1425, 872, and 710 cm^{-1} correspond to calcite and indicate asymmetric stretching, out-of-plane bending, and in-plane bending vibrations of the CO_3^{2-} groups, respectively. On the other hand, the peaks at 801 cm^{-1} and 437 cm^{-1} belong to scheelite (Dong et al., 2019; Dai et al., 2025; Chen et al., 2026). Calcite exhibits distinct bands at 2920 cm^{-1} and 2850 cm^{-1}, corresponding to asymmetric and symmetric CH_2 stretching vibrations, respectively, after treatment with oleic acid (Wang et al., 2020). Peaks at 1748 and 1820 cm^{-1} are attributed to the C=O stretching vibration of oleic acid (Wang et al., 2020; Wang et al., 2025), indicating the presence of a thin molecular layer of oleic acid on the surface of calcite, likely via weak chemisorption. In contrast, scheelite shows faint hydrocarbon stretching bands at 2920

cm^{-1} and 2850 cm^{-1}, and very weak C=O bands, implying much lower and weaker adsorption than in calcite.

Both scheelite and calcite showed CH_2 bands at 2908 and 2865 cm^{-1} when treated with palmitic acid. However, COO^- stretching bands with a doublet at 1540 and 1470 cm^{-1} were observed in the case of scheelite (Wang et al., 2025). It represents the ionization of palmitic acid and the formation of Ca-carboxylate complexes by coordination with Ca^{2+} ions, which are significant on the surface of scheelite. This demonstrates a stronger adsorption of palmitic acid on the scheelite surface than on calcite.

Moreover, in the presence of mixed collectors (oleic acid and palmitic acid at a ratio of 1:1), scheelite exhibits broader and deeper CH_2 stretching bands at 2868 and 2912 cm^{-1} along with carboxylate bands around 1550 cm^{-1} and 1410 cm^{-1} compared to the corresponding peaks of calcite. These IR results suggest that adsorption on the surface of scheelite is enhanced with a mixed collector system compared to calcite.

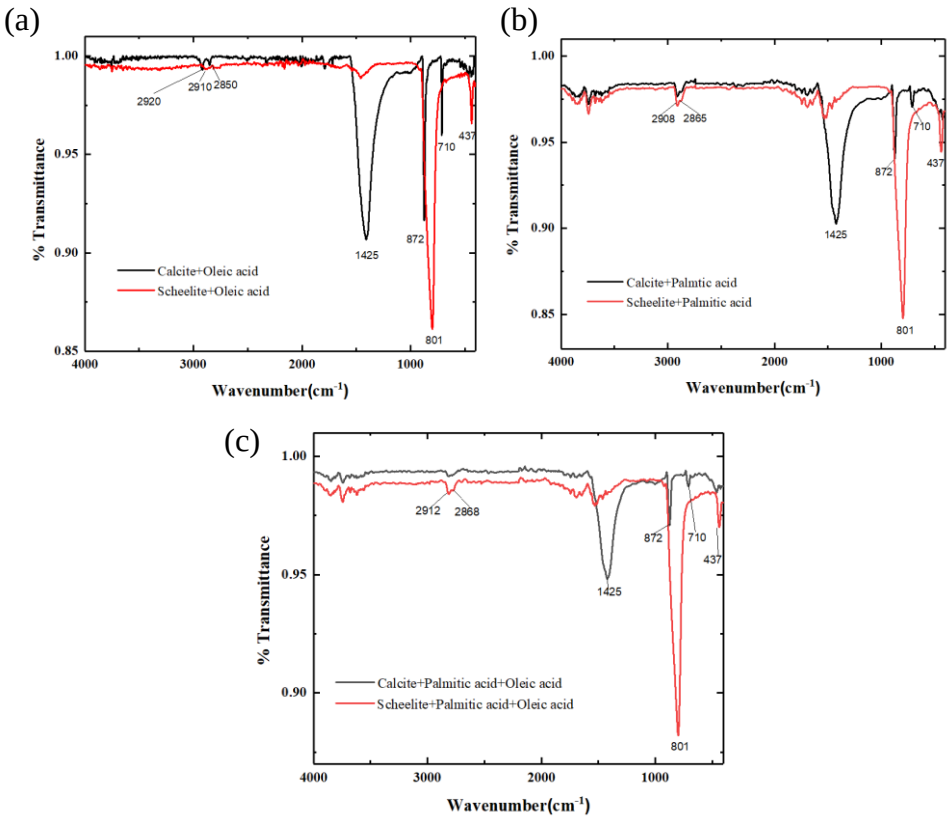

Fig. 9. FTIR spectra of (a) oleic acid with scheelite and calcite, (b) palmitic acid with scheelite and calcite, (c) 1:1 mixture of oleic acid and palmitic acid with scheelite and calcite

3.4. UV-Vis DRS analysis

The UV-Vis DRS spectrophotometer was employed to examine the surface electronic changes of scheelite and calcite before and after treatment with different collector systems. The corresponding spectra for scheelite and calcite are presented in Figs 10 and 11, respectively.

The UV-Vis spectrum of pristine scheelite exhibits a strong absorption band aroud 250 nm with in the UV region (200-300nm), which is attributed to $O^{2-} \rightarrow W^{6+}$ charge-transfer transition within the WO_4^{2-} tetrahedral units (Gao et al., 2021, Kowalkińska et al., 2021). The absorbance intensity showed a considerable increase after treatment with fatty acid collectors. This indicates additional ligand-to-metal charge-transfer (LMCT) transitions and a modification of the surface electronic environment, which could be due to the adsorption of carboxylate groups on the surface of scheelite (Arndt et al., 2019; Kowalkinska et al., 2021). Fig. 10 shows a sequential increase in absorbance intensity from the pristine scheelite to the scheelite-oleic acid system and then to the scheelite-palmitic acid system. However, the maximum absorbance intensity was recorded for the scheelite treated with a 1:1 mixture of oleic acid and palmitic acid, suggesting a stronger alteration of the surface electronic environment.

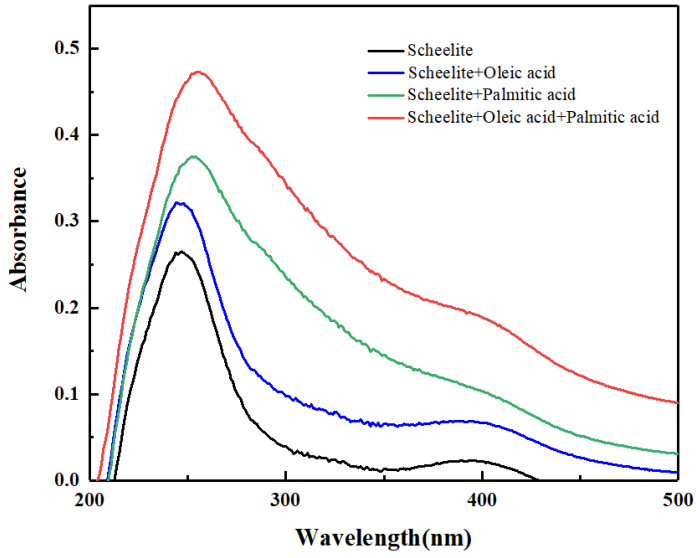

Fig. 10. UV-Vis DRS of scheelite and scheelite treated with collectors

Fig. 11 presents the UV-Vis DRS spectra of pristine calcite and after treatment with different fatty acid collectors. Calcite displayed a minimal absorbance within the 200–500 nm range, indicating the weak intrinsic electronic transitions of the $CaCO_3$ lattice (Sulimai et al., 2019).

Calcite exhibited a similar trend to scheelite, with absorbance intensity increasing from pristine calcite to treatment under the oleic acid system, then to the palmitic acid system, and reaching a maximum in the 1:1 mixture of oleic acid and palmitic acid. However, it is worth noting that the differences among these spectra are relatively less than those of scheelite. Moreover, these spectra tend to converge in the higher-wavelength region, unlike scheelite, indicating a relatively weaker alteration of the surface electronic environment. These observations elucidate that although fatty acids, especially the mixed collector system, adsorb on calcite, the extent of adsorption (alteration in surface electronic environment) is lower than that on scheelite, which aligns well with the flotation and FTIR results.

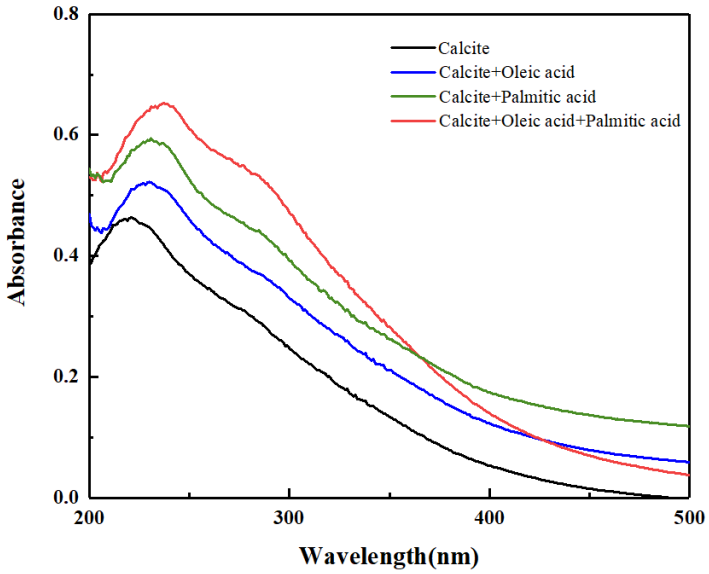

Fig. 11. UV-Vis DRS of calcite and calcite treated with different collectors

3.4. XPS analysis

XPS analysis was undertaken to elucidate the nature and strength of interaction between collector species and the mineral surfaces. It is instrumental in detecting the chemical state of mineral surface elements, thereby explaining the formation of new

surface species and their respective adsorption mechanisms (Jiao et al., 2019). In the present study, the O 1s and Ca 2p spectra of pristine scheelite and calcite were measured before and after adsorption under different collector systems, as shown in Figs. 12-15.

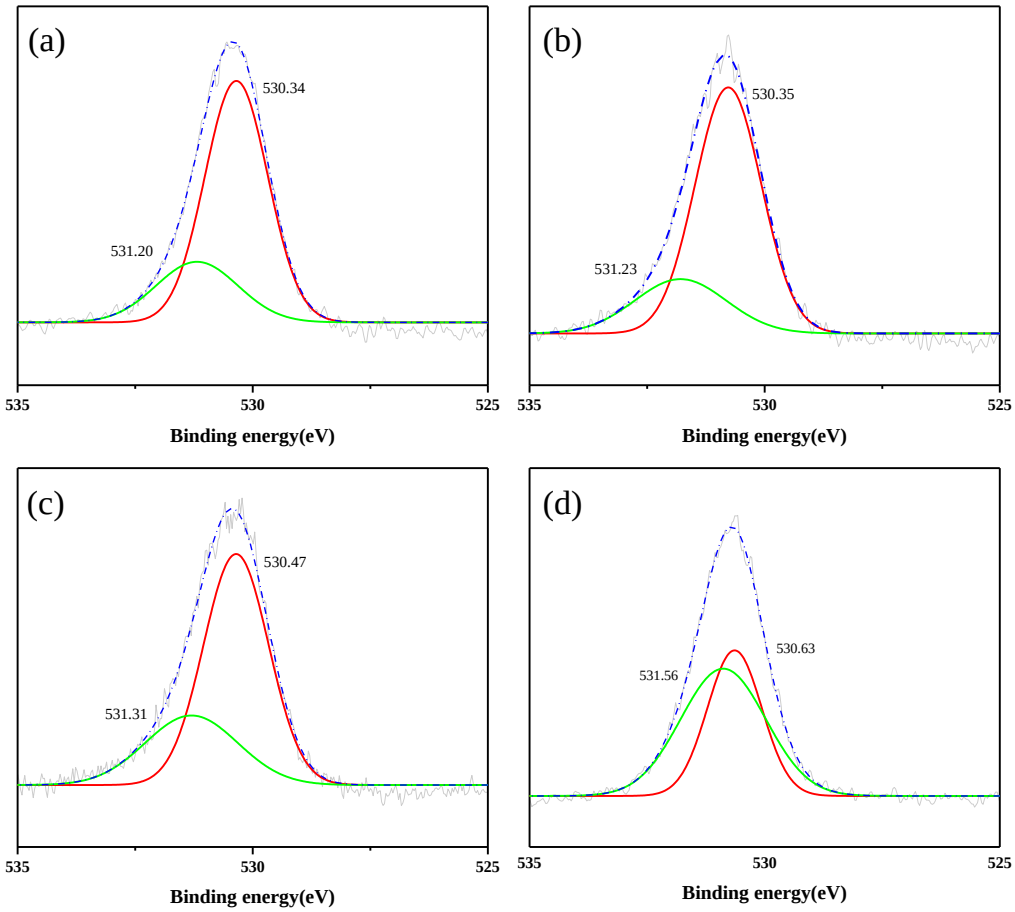

Fig. 12. O1s spectra of (a) scheelite, (b) scheelite + oleic acid, (c) scheelite + palmitic acid, (d) scheelite + oleic acid+ palmitic acid

The pristine scheelite surface is characterized by a dominant lattice-oxygen (WO_4^{2-}) peak at approximately 530.34 eV, accompanied by a small shoulder at 531.20 eV (Fig. 12a), which can be attributed to surface hydroxyl groups (Kuang et al., 2021). After the adsorption with oleic acid, the O1s peak was deconvoluted into two components at 530.35 and 531.23 eV, resulting in a shift of 0.01 and 0.03 eV from their corresponding peaks present in untreated scheelite (Fig. 12b). These minor changes are within the order of scan steps (0.05 eV), indicating weak adsorption.

Fig. 12c shows the O1s spectra of scheelite obtained after treatment with palmitic acid, where noticeable shifts of 0.13 and 0.11 eV in O1s peaks (at 530.47 and 531.31 eV) were observed. The relative increase in shifts with palmitic acid further confirms its superior selectivity towards scheelite compared to oleic acid. However, the maximum binding energy shift was observed for the 1:1 mixture of oleic and palmitic acid, where the deconvoluted peaks appeared at 530.63 and 531.56 with shifts of 0.29 and 0.36 eV (Fig. 12d). These shifts are significantly higher than the instrumental step size, indicating strong interaction with the scheelite surface. The survey spectrum correlates well with the flotation results and the FTIR analysis, confirming enhanced adsorption when using a mixed collector system.

Although calcite exhibited a similar overall trend, its peaks were chemically distinct due to the presence of carbonate lattice (Fig. 13). The pristine calcite surface showed a lattice-oxygen (CO_3^{2-}) peak around 531.24 eV along with a secondary peak at 532.32 eV (Liu et al., 2025). Fig. 13b shows that oleic acid adsorption shifted the O1s peaks to 531.30 and 532.40 eV, corresponding to increases of 0.06 and 0.08 eV, respectively. Notably, these shifts with calcite are higher than those of scheelite, indicating that oleic acid exhibits a stronger affinity towards calcite than scheelite.

Similarly, in the case of palmitic acid (Fig. 13c), the deconvolution of peaks was at 531.34 and 532.42 eV with the shifts of around 0.10 eV, which is slightly higher than those for oleic acid. It is worth noting that these shifts are considerably lower than those observed in scheelite, indicating a relatively weaker interaction with calcite. However, Fig. 13d shows that the O1S peaks shift to 531.51 and 532.62 eV (an increase of 0.27 and 0.30 eV) under the mixed collector system, confirming enhanced adsorption relative to individual collectors.

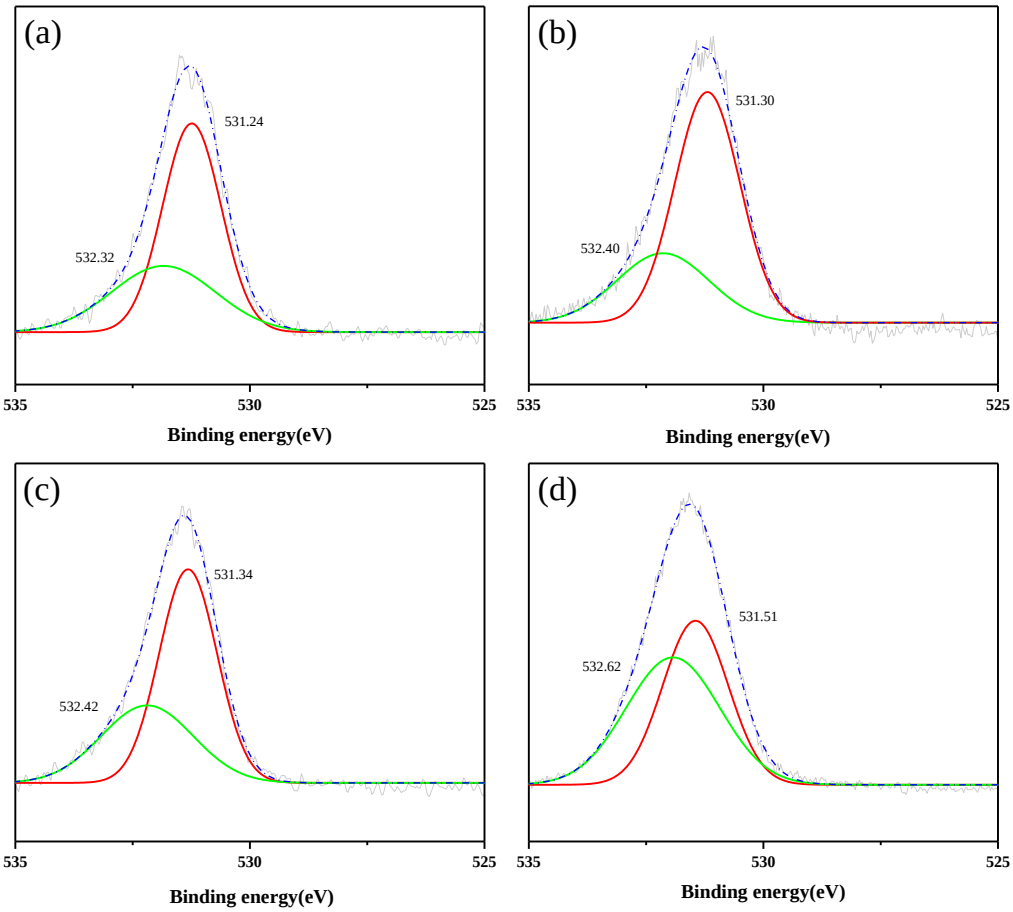

Fig. 13. O1s spectra of (a) Calcite, (b) calcite + oleic acid, (c) calcite + palmitic acid, (d) calcite + oleic acid + palmitic acid

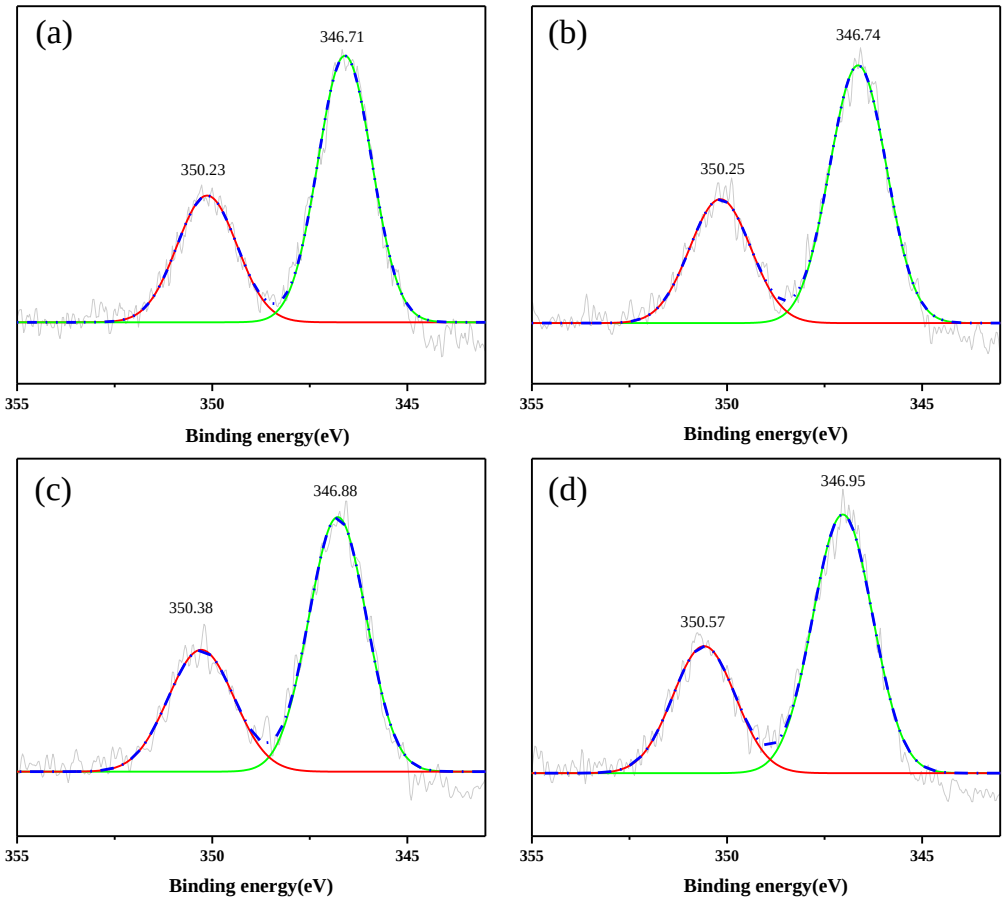

Fig. 14. Ca 2p spectra of (a) scheelite, (b) scheelite + oleic acid, (c) scheelite + palmitic acid, (d) scheelite + oleic acid+ palmitic acid

Fig. 14a shows the Ca 2p spectra of pristine scheelite, which exhibit the characteristic spin–orbit doublet Ca 2p3/2 and Ca 2p1/2 at 346.71 eV and 350.23 eV, respectively. This suggests the presence of Ca^{2+} in the lattice environment of scheelite (Gao et al, 2018). After treatment with oleic acid, the doublets appeared at 346.74 and 350.25 eV, with marginal shifts of 0.03 and 0.02 eV, respectively, indicating minor changes in the Ca chemical environment (Fig. 14b).

In contrast, treatment with palmitic acid exhibited considerable positive shifts in Ca 2p spectra of 0.17 and 0.15 eV (at 346.88 and 350.38 eV) indicating better adsorption by palmitic acid than oleic acid (Fig. 14c). Nevertheless, the most pronounced shifts of 0.24 and 0.19 eV were observed by 1:1 mixture of oleic and palmitic acid, with peaks located at 346.95 eV and 350.57 eV, respectively (Fig. 14d). Such increase in binding

energy shift signifies a stronger adsorption with surface Ca-sites of mixed collector system in compared to individual collectors.

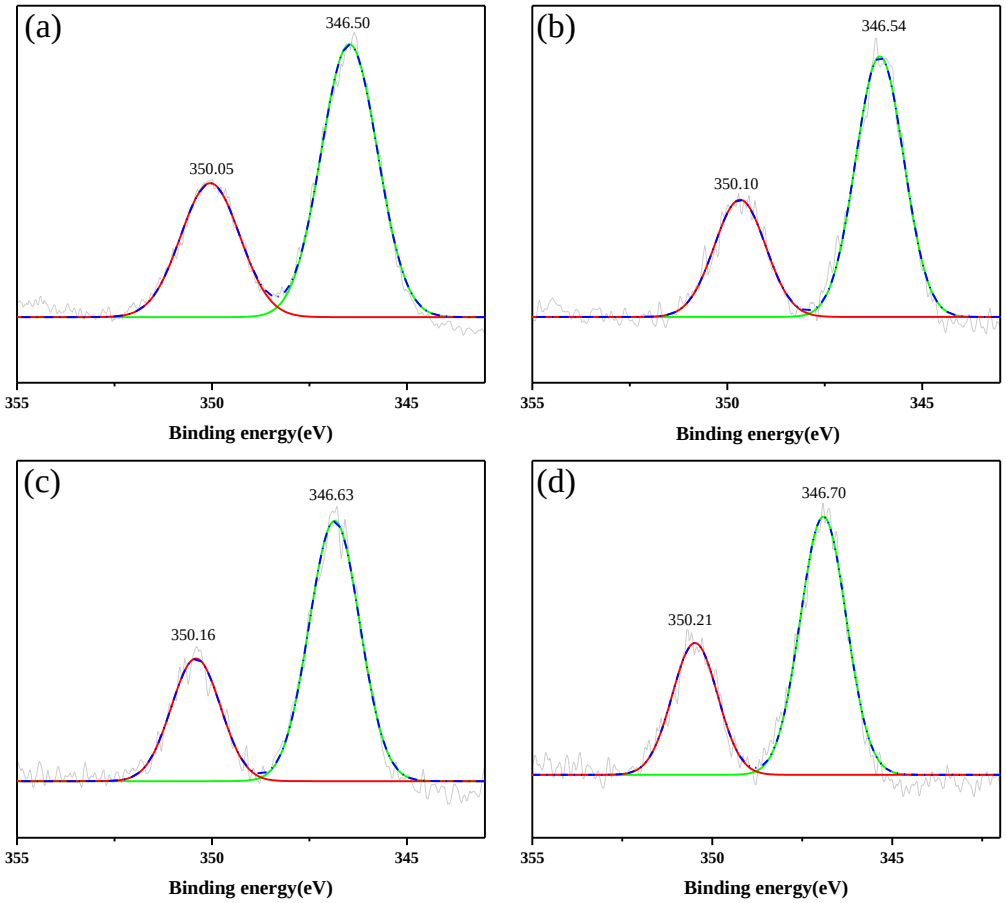

Fig. 15. Ca 2p spectra of (a) Calcite, (b) calcite + oleic acid, (c) calcite + palmitic acid, (d) calcite + oleic acid + palmitic acid

The high-resolution Ca 2p spectra (Fig. 15a) of pristine calcite exhibit the characteristic spin-orbit doublet with dominant component Ca $2p_{3/2}$ at 346.50 eV and Ca $2p_{1/2}$ at 350.05 eV (Guan et al., 2024). After treatment with oleic acid, the peaks were slightly shifted to 346.54 eV and 350.10 eV with positive shifts of 0.04 eV and 0.05 eV, respectively (Fig. 15b). Notably, the shifts in calcite are slightly higher than their corresponding shifts in the case of scheelite. However, adsorption with palmitic acid with calcite resulted relatively higher positive shifts of 0.13 eV and 0.11 eV of binding energy (at 346.63 eV and 350.16 eV), showcasing better adsorption than oleic acid (Fig. 15c). In case of mixed collector system, the Ca 2p peaks further shifted to 346.70 eV and 350.21 eV, corresponding to positive shifts of 0.20eV and 0.16 eV, respectively

(Fig. 15d). The increase in binding energy shift suggests stronger adsorption of mixed collector system over the individual collectors.

Overall, the Ca 2p spectra results support the interaction of the near-surface Ca sites linked to collector adsorption, while the shifting in binding-energy confirms that calcium is retained predominantly in Ca^{2+} state and no new Ca phase has been formed.

In order to quantify the extent of adsorption, a constant "*R*" was calculated, which can be defined as the ratio between the area of the high-binding-energy O 1s component and that of the lattice oxygen component as expressed in Equation 1. In the present investigation, only the O 1s spectra have been considered, as they directly reflect the increase in adsorbate-related oxygen due to adsorbed fatty acids. In contrast, Ca 2p spectra primarily reflect Ca^{2+}on the mineral surface, typically exhibiting a very small chemical shift, making it less sensitive in comparison to O 1s.

$$R = \frac{A_{HBE}}{A_{Lattice}} \qquad (1)$$

The "A_{HBE}" represents the area due to the high binding energy of O1s spectra. It is attributed to surface hydroxyl groups and carboxylate (COO-) groups, mainly due to collector adsorption. On the other hand, "$A_{lattice}$" corresponds to the area due to the inherent oxygen present in the mineral structure. Therefore, the ratio represented by "R" could serve to quantify the change and estimate the extent of collector adsorption. In view of this, the change in R ($\Delta R = R_{treated} - R_{pristine}$) before and after collector adsorption under different collector systems is presented in Table 2. It may be noted that the ratio (R) denotes relative adsorption on the scheelite and calcite surfaces rather than absolute quantification.

Table 2. Values of ΔR for scheelite and calcite under different collector systems

Minerals	ΔR	
Scheelite	Oleic acid	0.15
	Palmitic acid	0.29
	1:1 Mixture	0.81
Calcite	Oleic acid	0.19
	Palmitic acid	0.24
	1:1 Mixture	0.69

Table 2 demonstrates that the oleic acid and palmitic acid mixture (1:1) exhibits the highest ΔR values for both scheelite and calcite, signifying its superior adsorption on both the mineral surface compared to the individual collectors. However, the relatively higher ΔR value for scheelite (0.81) compared to calcite (0.69) indicates its superior selectivity towards scheelite, which is consistent with the flotation results.

3.6. MD simulations

Molecular dynamics simulations were performed on the scheelite (112) surface to gain molecular-level insights into the adsorption behaviour of palmitic acid, oleic acid, and their 1:1 mixture at the solid-liquid interface. Fig. 16 presents MD configurations for the adsorption of the scheelite (112) surface with different collector systems. In the pure scheelite-water system (Fig. 16a), a well-structured water layer is visible near the scheelite surface, depicting the hydrophilic nature of scheelite. Foucaud et al. (2022) studied the hydration mechanism of the scheelite (112) surface and reported the strong tendency for hydroxylation due to the adsorption of water molecules between two calcium atoms.

When collector molecules were introduced to the scheelite (112) surface (Fig. 16b, 16c & 16d), the collector molecules are seen getting adsorbed on the surface of scheelite, displacing the pre-adsorbed water molecules. Therefore, the concentration profiles of both water molecules and collector species near the scheelite surface could provide insights about the degree of adsorption and subsequent hydrophobicity imparted to the scheelite surface. Typically, collector adsorption on the mineral surface leads to the displacement of surface-bound water molecules; hence, a decrease in water density along with an increase in collector concentration provides a comparative measure of adsorption strength and selectivity. The resulting profiles are presented in Fig. 17 and 18, illustrating the concentration profiles of water and collector molecules, respectively, with different collector systems. The systems are denoted as W–S (water–scheelite), W–OA–S (oleic acid), W–PA–S (palmitic acid), and W–(OA+PA)–S (a 1:1 mixture of oleic and palmitic acid).

As shown in Fig. 17, the first hydration layer of water molecules forms at approximately 12–14 Å from the scheelite surface, regardless of the collector system.

However, the relative water density near the surface varies significantly among these systems and is found to be in the following order:

W–S > W–OA–S > W–PA–S > W–(OA+PA)–S

It indicates that the ability to displace pre-adsorbed water is highest for the oleic acid-palmitic acid mixture. Moreover, palmitic acid exhibits greater water-displacement ability than oleic acid, despite having a shorter carbon chain. This can be attributed to its saturated, linear hydrocarbon chain, which allows tighter packing and stronger lateral chain–chain interactions, thereby disrupting the hydration layer more effectively (Filippov et al., 2018). In contrast, the cis-double bond in the oleic acid molecule introduces a bend in the hydrocarbon chain. Moreover, oleic acid possesses higher water solubility than palmitic acid, which causes the formation of a more water-permeable adsorption layer than palmitic acid (Leja, 1981; Filippov et al., 2018).

The collector concentration profiles (Fig. 18) show that the adsorbed reagent layer forms at approximately 12–16 Å from the scheelite surface along the Z-axis. A slight rightward shift in the concentration peak is observed from the W–(OA+PA)–S system to the W–OA–S system, indicating that the adsorption layer formed by the mixed collectors lies closer to the mineral surface. Such a closer arrangement reflects stronger interaction between the scheelite surface and oleic acid-palmitic acid mixture, imparting maximum hydrophobicity.

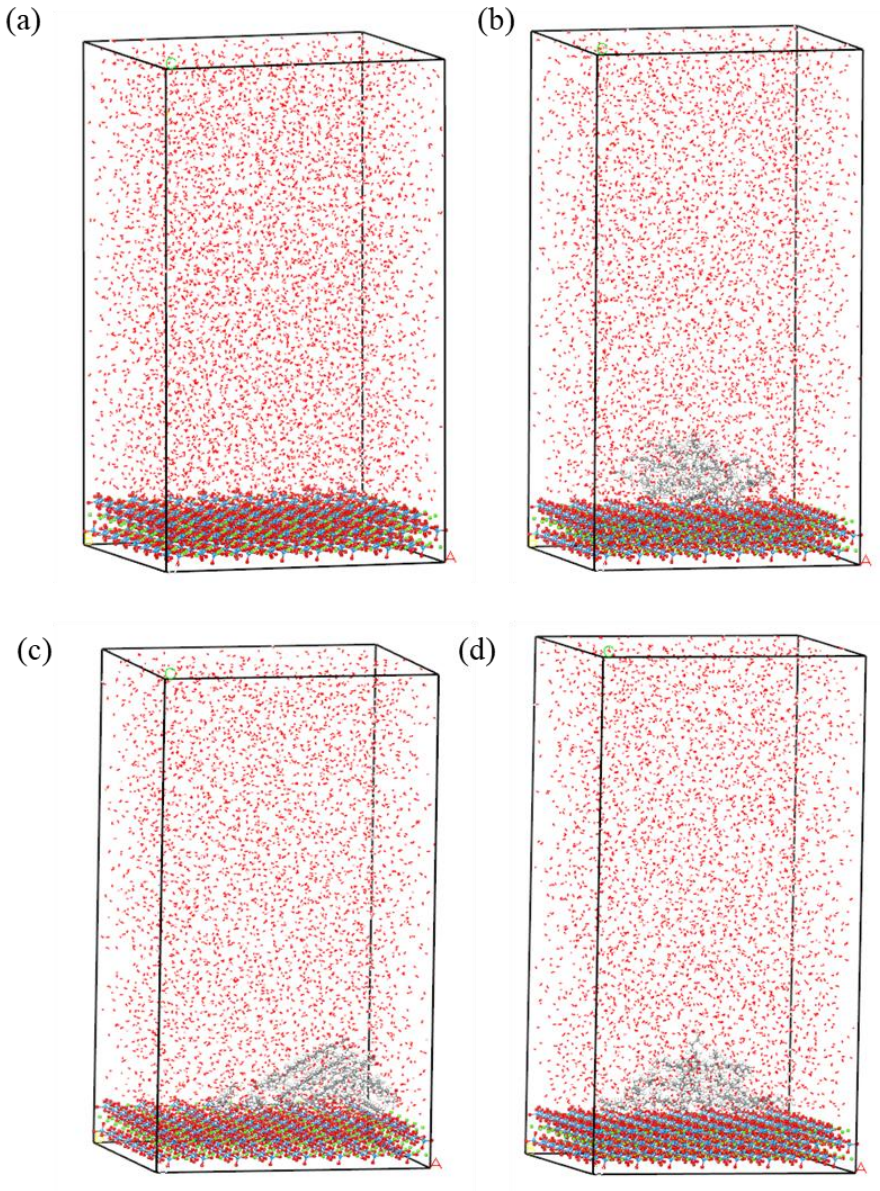

Fig. 16. MD configurations for the adsorption of scheelite (112) surface under different systems (a) scheelite-water, (b)scheelite-oleic acid-water, (c) scheelite-palmitic acid-water, (d) scheelite-oleic acid and palmitic acid mixture (1:1)-water

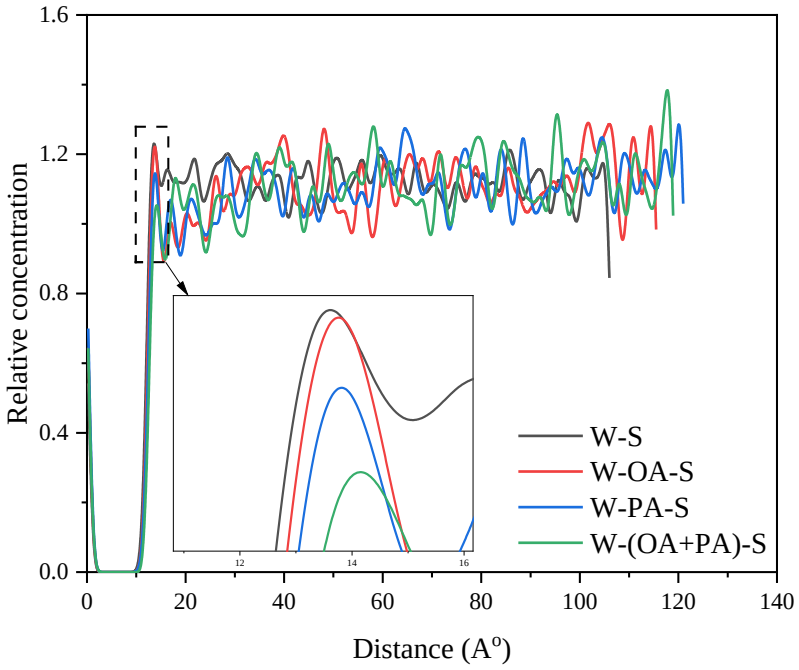

Fig. 17. Relative concentration of water molecules near the scheelite (112) surface under different systems

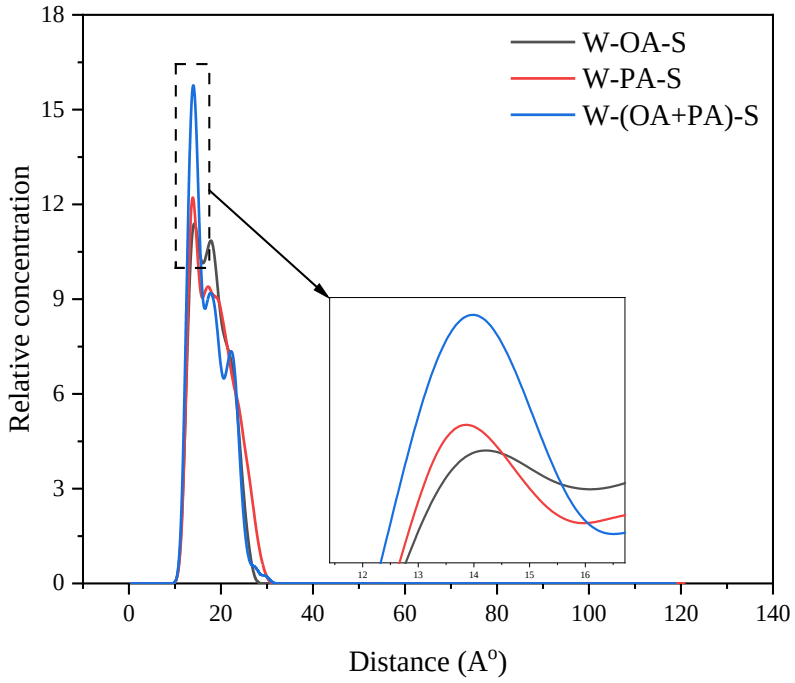

Fig. 18. Relative concentration of collector molecules under different collector systems

4. Conclusions

This work presented a novel and practical approach to the selective flotation of scheelite from calcite. It comprehensively examined the use of various fatty acids, including oleic acid, palmitic acid, mandelic acid, and myristic acid, as collectors in a scheelite-calcite flotation system. Experimental results demonstrated that the molecular structure, chain length, and degree of saturation of fatty acids significantly influence overall flotation performance. Oleic acid, being an unsaturated fatty acid, was found to be instrumental in achieving the maximum recovery, while saturated palmitic acid attained the highest grade. In view of this, the present study comprehensively investigated the use of oleic acid, palmitic acid, and their combination at various ratios to selectively float scheelite from calcite.

The flotation experimental results indicated that a 1:1 mixture of oleic acid and palmitic acid could achieve a WO_3 content of 2.2% at a recovery of approximately 81.2%, from a feed assaying about 0.19%. Meanwhile, calcite recovery decreased significantly to about 26.8%, demonstrating the superior selectivity of the mixed collector system for scheelite over calcite.

Furthermore, the FTIR, UV-Vis DRS, and XPS analyses of the reagents adsorbed on the pure mineral samples were well aligned with the flotation results. FTIR spectra confirmed that the 1:1 mixture of oleic acid and palmitic acid exhibited better adsorption on the scheelite surface compared to calcite. The -CH_2 stretching bands on scheelite, when treated with the mixed collectors, were deeper and broader than the corresponding peaks observed with individual collectors. The UV-Vis DRS observations also indicated that the mixed collector system has stronger adsorption characteristics on both scheelite and calcite. However, the extent of alteration in the surface electronic environment of calcite is relatively lower than that of scheelite. Similarly, the XPS analysis of the O 1s region showed the highest spectral contribution by mixed collector system on scheelite. This further confirmed that the mixed collector system imparts stronger adsorption on scheelite compared to calcite.

Additionally, MD simulations provided insight into the interaction between collector molecules and mineral surfaces. The concentration profiles of collector species and

water molecules indicated that the 1:1 mixture of oleic acid and palmitic acid exhibited the maximum water-displacing ability, as well as accumulated the highest number of collector molecules near the scheelite (112) surface, facilitating adequate flotation of scheelite.

Declaration of Interest

The authors declare that they have no known competing financial interests or personal relationships that could have appeared to influence the work reported in this paper.

Acknowledgement

The authors are grateful to the Director of the CSIR-Institute of Minerals and Materials Technology, Bhubaneswar, for his kind consent to publish this article.

References

[1] Z. Zhu, J. Qi, X. Tong, Z. Cai, Strengthening the flotation enrichment of scheelite with an amino-hydroxamate collector, Applied Surface Science 708 (2025) 163761. https://doi.org/10.1016/j.apsusc.2025.163761.

[2] X. Yang, Beneficiation studies of tungsten ores – A review, Minerals Engineering 125 (2018) 111–119. https://doi.org/10.1016/j.mineng.2018.06.001.

[3] Q. Wu, Y. Zhu, W. Sun, R. Xie, Y. Li, Y. Han, Adsorption mechanism of efficient flotation separation of scheelite from calcite by a novel mixed collector, Journal of Molecular Liquids 345 (2022) 116994. https://doi.org/10.1016/j.molliq.2021.116994.

[4] Z. Wei, W. Sun, H. Han, X. Gui, Y. Xing, Flotation chemistry of scheelite and its practice: A comprehensive review, Minerals Engineering 204 (2023) 108404. https://doi.org/10.1016/j.mineng.2023.108404.

[5] Z. Wang, H. Wu, Y. Xu, K. Shu, S. Fang, L. Xu, The effect of dissolved calcite species on the flotation of bastnaesite using sodium oleate, Minerals Engineering 145 (2020) 106095. https://doi.org/10.1016/j.mineng.2019.106095.

[6] X. Wang, Y. Cui, Mechanism of flotation separation of scheelite from calcite using sulfonated phenolic resin as a novel depressant, Minerals

Engineering 230 (2025) 109393. https://doi.org/10.1016/j.mineng.2025.109393.

[7] N.H. Sulimai, R.A. Rani, Z. Khusaimi, S. Abdullah, M.J. Salifairus, S. Alrokayan, H. Khan, P.A. Sermon, M. Rusop, Facile synthesis of CaCO3 and investigation on structural and optical properties of high purity crystalline calcite, Materials Science and Engineering: B 243 (2019) 78–85. https://doi.org/10.1016/j.mseb.2019.03.006.

[8] L.H. Santos, G. Otávio Dos Santos, L. Fernandes De Magalhães, G. Rodrigues Da Silva, A. Eduardo Clark Peres, Application of andiroba oil as a novel collector in apatite flotation, Minerals Engineering 185 (2022) 107678. https://doi.org/10.1016/j.mineng.2022.107678.

[9] T. Peng, L. Tao, J. Wang, L. Dong, W. Jia, F. Wang, J. Hu, Z. Gao, Selective flotation separation of scheelite from calcite using hexamethylenediamine tetramethylene phosphonic acid as a novel depressant, Journal of Molecular Liquids 402 (2024) 124569. https://doi.org/10.1016/j.molliq.2024.124569.

[10] P.D. Oliveira, H. Mansur, A. Mansur, G.D. Silva, A.E. Clark Peres, Apatite flotation using pataua palm tree oil as collector, Journal of Materials Research and Technology 8 (2019) 4612–4619. https://doi.org/10.1016/j.jmrt.2019.08.005.

[11] M. Liu, X. Wu, G. Li, C. Liu, Z. Ma, Y. Guo, J. Tian, D. Wang, K. Shu, Z. Wang, L. Xu, Selective adsorption mechanism of a novel hydroxamic acid containing a thioether group collector for flotation separation of bastnaesite from calcite, Chemical Engineering Science 312 (2025) 121667. https://doi.org/10.1016/j.ces.2025.121667.

[12] S. Li, Y. Zhu, J. Liu, Y. Wang, Y. Han, Flotation separation of spodumene from beryl or gangue (albite and quartz) with α-bromo-myristic acid as a collector, Minerals Engineering 228 (2025) 109329. https://doi.org/10.1016/j.mineng.2025.109329.

[13] J. Leja, Surface Chemistry of Froth Flotation, Springer US, Boston, MA, 1981. https://doi.org/10.1007/978-1-4615-7975-5.

[14] N. Kupka, M. Rudolph, Froth flotation of scheelite – A review, International Journal of Mining Science and Technology 28 (2017) 373–

384. https://doi.org/10.1016/j.ijmst.2017.12.001.

[15] J. Kuang, Z. Zou, Z. Huang, P. Liu, W. Yuan, L. Zhu, Surface dissolution of scheelite under different regulators and its effect on flotation behavior, Minerals Engineering 164 (2021) 106811. https://doi.org/10.1016/j.mineng.2021.106811.

[16] M. Kowalkińska, P. Głuchowski, T. Swebocki, T. Ossowski, A. Ostrowski, W. Bednarski, J. Karczewski, A. Zielińska-Jurek, Scheelite-Type Wide-Bandgap ABO_4 Compounds (A = Ca, Sr, and Ba; B = Mo and W) as Potential Photocatalysts for Water Treatment, J. Phys. Chem. C 125 (2021) 25497–25513. https://doi.org/10.1021/acs.jpcc.1c06481.

[17] B. Kawenski Cook, M. Aghamirian, C.E. Gibson, Optimization of spodumene flotation with a fatty acid collector, Minerals Engineering 204 (2023) 108412. https://doi.org/10.1016/j.mineng.2023.108412.

[18] J. Kang, S.A. Khoso, Y. Hu, W. Sun, Z. Gao, R. Liu, Utilisation of 1-Hydroxyethylidene-1, 1-diphosphonicacid as a selective depressant for the separation of scheelite from calcite and fluorite, Colloids and Surfaces A: Physicochemical and Engineering Aspects 582 (2019) 123888. https://doi.org/10.1016/j.colsurfa.2019.123888.

[19] F. Jiao, L. Dong, W. Qin, W. Liu, C. Hu, Flotation separation of scheelite from calcite using pectin as depressant, Minerals Engineering 136 (2019) 120–128. https://doi.org/10.1016/j.mineng.2019.03.019.

[20] Q. He, Z. Guan, Y. Zhang, Z. Zhang, W. Dai, Y. Wu, Novel eco-friendly depressant sodium bis(1,6-hexamethylenetriamine pentamethylenephosphonate) for efficient flotation separation of scheelite and calcite, Colloids and Surfaces A: Physicochemical and Engineering Aspects 726 (2025) 137947. https://doi.org/10.1016/j.colsurfa.2025.137947.

[21] H. Han, W. Liu, Y. Hu, W. Sun, X. Li, A novel flotation scheme: selective flotation of tungsten minerals from calcium minerals using Pb–BHA complexes in Shizhuyuan, Rare Metals 36 (2017) 533–540. https://doi.org/10.1007/s12598-017-0907-8.

[22] Z. Guan, Y. Zhang, S. Wen, Y. Wu, X. Li, X. Li, Mn-SS as a novel depressant of the flotation process of scheelite and calcite: Role and

mechanism, Colloids and Surfaces A: Physicochemical and Engineering Aspects 686 (2024) 133443. https://doi.org/10.1016/j.colsurfa.2024.133443.

[23] Z. Guan, R. Liao, Q. Zuo, Y. Wu, Y. Zhang, S. Wen, Mechanistic analysis and validation of an efficient novel inhibitor for scheelite and calcite flotation separation: A DFT and MD simulation study, Applied Surface Science 662 (2024) 160146. https://doi.org/10.1016/j.apsusc.2024.160146.

[24] Z. Gao, Y. Hu, W. Sun, J.W. Drelich, Surface-Charge Anisotropy of Scheelite Crystals, Langmuir 32 (2016) 6282–6288. https://doi.org/10.1021/acs.langmuir.6b01252.

[25] Z. Gao, J. Deng, W. Sun, J. Wang, Y. Liu, F. Xu, Q. Wang, Selective Flotation of Scheelite from Calcite Using a Novel Reagent Scheme, Mineral Processing and Extractive Metallurgy Review 43 (2022) 137–149. https://doi.org/10.1080/08827508.2020.1825956.

[26] Y. Gao, Z. Gao, W. Sun, Z. Yin, J. Wang, Y. Hu, Adsorption of a novel reagent scheme on scheelite and calcite causing an effective flotation separation, Journal of Colloid and Interface Science 512 (2018) 39–46. https://doi.org/10.1016/j.jcis.2017.10.045.

[27] G. Gao, Z. Geng, G. Li, Z. Tan, Y. Lu, Z. Fan, Q. Wang, L. Li, Understanding the Doping Chemistry of High Oxidation States in Scheelite $CaWO_4$ by Hydrothermal Conditions, Inorg. Chem. 60 (2021) 16558–16569. https://doi.org/10.1021/acs.inorgchem.1c02450.

[28] Y. Foucaud, L. Filippov, I. Filippova, M. Badawi, The Challenge of Tungsten Skarn Processing by Froth Flotation: A Review, Front. Chem. 8 (2020) 230. https://doi.org/10.3389/fchem.2020.00230.

[29] Y. Foucaud, A. Collet, I.V. Filippova, M. Badawi, L.O. Filippov, Synergistic effects between fatty acids and non-ionic reagents for the selective flotation of scheelite from a complex tungsten skarn ore, Minerals Engineering 182 (2022) 107566. https://doi.org/10.1016/j.mineng.2022.107566.

[30] Y. Foucaud, R.L.S. Canevesi, A. Celzard, V. Fierro, M. Badawi, Hydration mechanisms of scheelite from adsorption isotherms and ab initio

molecular dynamics simulations, Applied Surface Science 562 (2021) 150137. https://doi.org/10.1016/j.apsusc.2021.150137.

[31] Y. Foucaud, M. Badawi, L. Filippov, I. Filippova, S. Lebègue, A review of atomistic simulation methods for surface physical-chemistry phenomena applied to froth flotation, Minerals Engineering 143 (2019) 106020. https://doi.org/10.1016/j.mineng.2019.106020.

[32] L.O. Filippov, I.V. Filippova, Z. Lafhaj, D. Fornasiero, The role of a fatty alcohol in improving calcium minerals flotation with oleate, Colloids and Surfaces A: Physicochemical and Engineering Aspects 560 (2019) 410–417. https://doi.org/10.1016/j.colsurfa.2018.10.022.

[33] L.O. Filippov, Y. Foucaud, I.V. Filippova, M. Badawi, New reagent formulations for selective flotation of scheelite from a skarn ore with complex calcium minerals gangue, Minerals Engineering 123 (2018) 85–94. https://doi.org/10.1016/j.mineng.2018.05.001.

[34] L. Dong, F. Jiao, W. Qin, W. Liu, Selective flotation of scheelite from calcite using xanthan gum as depressant, Minerals Engineering 138 (2019) 14–23. https://doi.org/10.1016/j.mineng.2019.04.030.

[35] L. Dong, F. Jiao, W. Qin, H. Zhu, W. Jia, Effect of acidified water glass on the flotation separation of scheelite from calcite using mixed cationic/anionic collectors, Applied Surface Science 444 (2018) 747–756. https://doi.org/10.1016/j.apsusc.2018.03.097.

[36] P. Dhar, M. Thornhill, H.R. Kota, An Overview of Calcite Recovery by Flotation, Mater Circ Econ 2 (2020) 9. https://doi.org/10.1007/s42824-020-00006-y.

[37] S.K. Das, J. Tan, T. Kundu, S.S. Rath, Shivakumar.I. Angadi, Performance evaluation of Falcon fluidized bowl and ultrafine (UF) bowl concentrators for the recovery of ultrafine scheelite particles, Advanced Powder Technology 34 (2023) 104193. https://doi.org/10.1016/j.apt.2023.104193.

[38] S.K. Das, S.S. Rath, T. Kundu, N. Dash, S.I. Angadi, Decoding the beneficiation of ultra-fine scheelite values from gold mine tailings: mineralogical investigation and flowsheet development, Separation Science and Technology 60 (2025) 797–811.

https://doi.org/10.1080/01496395.2025.2457424.

[39] S.K. Das, C.H.R.V.S. Nagesh, T. Sreenivas, T. Kundu, S.I. Angadi, A treatise on occurrence, beneficiation and plant practices of tungsten-bearing ores, Powder Technology 429 (2023) 118938. https://doi.org/10.1016/j.powtec.2023.118938.

[40] S.K. Das, T. Kundu, N. Dash, S.I. Angadi, Separation behavior of Falcon concentrator for the recovery of ultrafine scheelite particles from the gold mine tailings, Separation and Purification Technology 309 (2023) 123065. https://doi.org/10.1016/j.seppur.2022.123065.

[41] L. Dai, B. Feng, W. Zhang, W. Guo, Study of the effect and mechanism of environmentally friendly depressant tragacanth gum on scheelite and apatite separation, Process Safety and Environmental Protection 196 (2025) 106913. https://doi.org/10.1016/j.psep.2025.106913.

[42] J. Chen, P. Gao, J. Liu, X. Wang, Y. Zhu, S. Yuan, Selective adsorption mechanism of a modified oleic-acid surfactant at scheelite–calcite surfaces, Colloids and Surfaces A: Physicochemical and Engineering Aspects 729 (2026) 138908. https://doi.org/10.1016/j.colsurfa.2025.138908.

[43] J. Chen, P. Gao, J. Liu, Y. Zhu, R. Xie, S. Yuan, Separating scheelite from calcite by a new high-selective collector of modified oleic acid and its mechanism, Applied Surface Science 701 (2025) 163292. https://doi.org/10.1016/j.apsusc.2025.163292.

[44] B. Arndt, K. Sellschopp, M. Creutzburg, E. Grånäs, K. Krausert, V. Vonk, S. Müller, H. Noei, G.B.V. Feldbauer, A. Stierle, Carboxylic acid induced near-surface restructuring of a magnetite surface, Commun Chem 2 (2019) 92. https://doi.org/10.1038/s42004-019-0197-1.

[45] M. Segall, M. Probert, C. Pickard, P. Hasnip, S. Clark, K. Refson, J. R. Yates, A. Bartok-Partay, M. Payne, Materials Studio CASTEP version 2024, Ab Initio Total Energy Program.

[46] S. J. Clark, M. D. Segall, C. J. Pickard, P. J. Hasnip, M. J. Probert, K. Refson, M. C. Payne, First principles methods using CASTEP, Zeitschrift fuer Kristallographie, (2005),220(5-6) p. 567-570.